Reconciliation of measured fully differential single ionization data with the first Born approximation convoluted with elastic scattering

M. Schulz,[1] M. Dürr,[2] B. Najjari,[2] R. Moshammer,[2] and J. Ullrich[2]
[1]*Physics Department and LAMOR, University of Missouri-Rolla, Rolla, Missouri 65409, USA*
[2]*Max-Planck-Institut für Kernphysik, Saupfercheckweg 1, 69117 Heidelberg, Germany*
(Received 2 July 2007; published 19 September 2007)

An analysis of experimental fully differential data for single ionization in 100 MeV/amu C^{6+}+He collisions is reported. We present a convolution of the first Born approximation with elastic scattering by using an event generator technique. Furthermore, the calculation is convoluted with all known experimental resolutions. Our analysis shows that elastic scattering is a viable explanation for surprising structures observed in the fully differential cross sections outside the scattering plane. Furthermore, it may even explain discrepancies in the "recoil peak" frequently observed for both ion and electron impact.

DOI: 10.1103/PhysRevA.76.032712 PACS number(s): 34.50.Fa, 07.05.Tp, 52.20.Hv

I. INTRODUCTION

Fully differential measurements on single ionization of atoms by charged-particle impact have proven to provide rich information about the reaction dynamics in fundamental few-body systems [1,2]. In the case of electron impact most such experiments were performed by measuring the ejected and scattered electrons in coincidence (e.g., Refs. [3–5]) and in the case of ion impact by measuring the recoil ions in coincidence with either the ejected electron (e.g., Refs. [6,7]) or the scattered projectile [8]. All detected particles were momentum analyzed and the momentum of the undetected third particle was deduced from momentum conservation.

The momentum spectrometers involving recoil-ion detection (COLTRIMS or reaction microscopes) have the crucially important feature that the particles are detected essentially with a 4π solid angle (the exact values vary with operation parameters). As a result, fully differential cross sections (FDCS) can be measured with high efficiency for the entire three-dimensional space and covering a large fraction of the phase space simultaneously. Such three-dimensional FDCS revealed that our understanding of single ionization by charged-particle impact may not be as complete as previously assumed based on FDCS measurements with restricted detection geometry [6,9]. Even for small perturbation η (projectile charge to velocity ratio), which is generally considered a relatively "easy" case, significant discrepancies between experiment and state-of-the-art calculations were observed. While for electrons ejected into the scattering plane (defined by the initial and final projectile momenta) theory was in reasonable agreement with the data, pronounced peak structures in the plane perpendicular to the scattering plane and containing the initial projectile beam axis could not even be qualitatively reproduced by the calculations.

Various explanations for the peak structures in the perpendicular plane and the failure of theory to reproduce them were offered. One suggested that elastic scattering between the projectile and the target core, known to be important to understand the projectile deflection at large scattering angles [10], transfers part of the flux in the binary and recoil peaks, well established structures occurring in the scattering plane, to the perpendicular plane [6]. The failure of the three-particle distorted wave (3DW) approach, which accounts for elastic scattering in the final-state wave function, to reproduce the data in the perpendicular plane was attributed to the fact that the 3DW wave function is not exact when all three collision fragments are close together [11,12]. Other higher-order calculations did reveal out-of-plane structures, but, exactly opposite to the observation, yielded a minimum rather than a maximum [13]. Based on their classical trajectory Monte Carlo (CTMC) calculation Fiol and Olson argued that the peak structure in the perpendicular plane is due to elastic scattering between the ejected electron and the residual target ion following the primary ionizing interaction between the projectile and the electron [14].

More recently, Fiol *et al.* suggested that the peak structure in the perpendicular plane is entirely due to the experimental resolution [15] (to some extent in contradiction to their earlier analysis, where such a peak structure was obtained with a CTMC calculation without accounting for the resolution [14]). Using an extensive Monte Carlo event generator (MCEG) method, where all known effects due to the resolution were consistently incorporated, we recently demonstrated that although the resolution indeed affects the FDCS in the perpendicular plane it can only account for at most 50% of the peak structure [16]. In that work a first Born approximation (FBA) calculation was convoluted with the experimental resolution as follows: first, an event file consisting of the three momentum components of the collision fragments was generated for 10^6 ionization events using a Monte Carlo method, such that the momentum distribution of these events reflects the FDCS calculated with the FBA. Second, the experimental resolution for each momentum component was added event by event using a random generator providing a Gauss distribution. Third, with these momenta, now afflicted with the resolution, the FDCS were analyzed exactly the same way as the experimental data.

The Monte Carlo event generator technique, well-known from elementary particle physics, is very powerful because it allows performing the convolution repeatedly and event-by-event only requiring the last two steps in the outline given above. The time-consuming and computer-intensive step is the generation of the event file. Sorting the events into the

spectra of interest only takes about one minute. Therefore, once the event file is generated the effect of the resolution can be tested very efficiently and systematically merely by varying the parameters determining the resolution and without having to generate a new event file. More importantly, this technique is not just limited to convoluting the primary calculation with the experimental resolution. It is also possible to convolute it with true physics effects not accounted for in the calculation, at least in an approximate manner. It thus offers a handy method to qualitatively, systematically, and relatively quickly test the impact of certain physical effects on a theoretical model originally not containing these effects. This can be particularly useful for experimentalists to analyze and interpret measured data.

Here we report on an approximate method to convolute the FBA with classical elastic scattering between the projectile and the target core using the MCEG technique. The goal is to obtain an estimate of the effects due to elastic scattering on the FDCS, especially in the perpendicular plane. Because of the limitations of our model, which will be discussed below, it is not intended to represent a full-fledged theoretical analysis and no conclusions on a quantitative level will be drawn. Nevertheless, considering these limitations we obtain surprisingly good agreement with the experimental data. We take this as further support that our original interpretation for the origin of the peak structure in the perpendicular plane [6] represents a viable explanation.

II. EXPERIMENTAL SETUP AND RESOLUTION

The experimental procedure has been discussed in detail earlier [16] and only a brief summary is provided here. The experiment was performed at GANIL in Caen, France. A 100 MeV/amu C^{6+} ion beam was intersected with a very cold ($\approx$1.5 K) beam of He atoms from a supersonic jet. The recoiling target ions and the ionized electrons were extracted in the longitudinal direction (defined by the projectile direction) by a weak electric field and detected by two-dimensional position sensitive channel plate detectors. A uniform magnetic field of 19 G confined the transverse motion of the electrons so that all electrons with a transverse momentum of less than 3 a.u. hit the detector. Both particles were measured in coincidence with the projectiles which did not change charge state. The transverse momenta of the recoil ion and the electron were obtained from the position information of the detectors. The longitudinal momentum component was determined from the time of flight of each particle from the collision region to the respective detector obtained from the coincidence times. The momentum vector of the scattered projectile was deduced from momentum conservation.

As discussed in detail previously, the transverse recoil-ion momentum resolution is mostly determined by the projectile beam size in the target region and by the temperature of the target beam [16]. Earlier we reported upper limit values of 1 mm$\times$1 mm for the beam size and 2 K for the temperature. These numbers were obtained by analyzing the widths of the momentum transfer spectra for the two transverse components. After further analysis, we can now provide more realistic estimates for the actual values. Information about the beam size is contained in the electron spectra. The magnetic field of the spectrometer forces the electrons into cyclotron motion. After a time of flights t_e equal to integral multiples of the cyclotron period T the electrons return to the projectile beam axis, which we use to define the origin of the coordinate system for the electron position spectrum. For these times the distance d of the electrons from the origin is therefore zero for infinitely good resolution. As a result, pronounced nodes are observed in a plot of d versus t_e, which, however, do not go to $d=0$ at $t_e=nT$ (where n is an integer number) because of the finite position resolution. With the MCEG technique we can systematically study the effect of the overall electron position resolution on the shape of the nodes. From this analysis we estimate the projectile beam size to be about 0.5 mm$\times$0.5 mm.

The temperature of the target beam in the y direction (defined by the target beam axis) is much larger than in the x and z direction [16]. We can therefore estimate the contribution of the temperature to the recoil-ion momentum resolution in the y direction from the difference in width of the momentum transfer spectra in the x and y directions using Gaussian error propagation and we find a value of about 1.5 K. In the longitudinal and x directions the temperature is less than 0.2 K. In the former, the beam size does not contribute to the momentum resolution because of the time-focusing configuration of the spectrometer [16]. These numbers result in recoil-ion momentum resolutions of $\Delta p_{recx}=0.23$ a.u. full width at half maximum (FWHM), $\Delta p_{recy}=0.46$ a.u. FWHM, and $\Delta p_{recz}=0.15$ a.u. FWHM. The resolution for the transverse momentum $p_{rect}=\sqrt{(p_{recx}^2+p_{recy}^2)}$ is given by the average of the resolutions in the x and y directions, i.e., $\Delta p_{rect}=0.35$ a.u. FWHM. The corresponding resolutions of the electrons depend on their momentum components. The average values of about $\Delta p_{elt}=0.1$ a.u. FWHM and $\Delta p_{elz}=0.01$ a.u. FWHM are considerably better than for the recoil ions.

III. CONVOLUTION OF THE FBA WITH CLASSICAL ELASTIC SCATTERING

A detailed description of the MCEG technique used in our analysis was reported recently [16] and will not be repeated here. Since this event file is based on the FBA, momentum exchange among the collision fragments can only occur through an interaction of the electron with either the projectile or the target core. Elastic scattering between the projectile and the recoil ion, in other words, is not included in this approximation. In this paper, we account for elastic scattering by adding event by event to the projectile momentum transfer and to the recoil-ion momentum obtained from the FBA an appropriate amount of momentum determined from the impact parameter dependent cross section as outlined below.

Classically, the momentum $\mathbf{q}_{es}$ transferred in elastic scattering between two particles is unambiguously determined by the impact parameter b and for an unscreened Coulomb potential this relation (in atomic units) is

$$q_{es} = 2Z_1Z_2/(bv_o), \tag{1}$$

where Z_1 and Z_2 are the nuclear charges of the projectile and the target and v_o is the projectile speed. The screening of the target nucleus by the passive electron we account for by introducing the b-dependent effective target charge

$$Z_2 = 1 + (1 + \alpha b)e^{-2\alpha b}. \tag{2}$$

For $\alpha = 1.665$ a very good fit of the potential between the projectile and the target to a Hartree-Fock potential is obtained [17] and we therefore use this parameterization of Z_2 in Eq. (1).

The impact parameter distribution of the incoming projectiles causing single ionization dN_I/db is proportional to the single ionization cross section differential in b,

$$dN_I/db \sim d\sigma/db = 2\pi bP(b), \tag{3}$$

where $P(b)$ is the impact parameter-dependent single ionization probability. $bP(b)$ was calculated with a continuum distorted wave—eikonal initial state (CDW-EIS) [18] and a time-dependent coupled channel (TDCC) [19] calculation, which yield similar, but not identical results. However, since we need to add the momentum transferred in elastic scattering event by event, these theoretical values cannot be used directly in our convolution. Instead, we simulated the calculated $bP(b)$ by a convolution of two uniform random distributions between 0 and 1. A good simulation is found for the following relation between the impact parameter and these random numbers R_1 and R_2,

$$b = b'(1 + e^{-6.5/b'}) \tag{4a}$$

with

$$b' = \sqrt{(b_1 + b_2)} \tag{4b}$$

and

$$b_i = -\ln(1 - R_i)R_i/[a(1 - R_i^2)], \quad i = 1,2. \tag{4c}$$

Here, a is a parameter which determines the location of the maximum in $bP(b)$ and for $a = 0.5$ the theoretical location ($b = 0.9$ a.u.) is reproduced.

Equations (4a)–(4c) were obtained partly analytically and partly by "trial and error." The impact parameter distribution dN_I/db is related to the random distribution dN_I/dR=constant through the chain rule so that, along with the proportionality (3), we obtain

$$dN_I/db = (dN_I/dR)(dR/db) \sim dR/db \sim bP(b) \tag{5}$$

$$\text{or} \quad R \sim \int bP(b)db.$$

Since the exact analytic dependence of the theoretical $bP(b)$ is not known the integral in Eq. (5) can only be evaluated approximately. The resultant dependence $b(R)$ can then be optimized by adjusting it to yield the best fit of the theoretical $bP(b)$. The simulated $bP(b)$ using this procedure is shown in Fig. 1 for $a = 0.5$ (solid curve) and for $a = 1.0$ (dash-dotted curve) in comparison with the CDW-EIS (dotted curve) and the TDCC (dashed curve) calculations. For all b

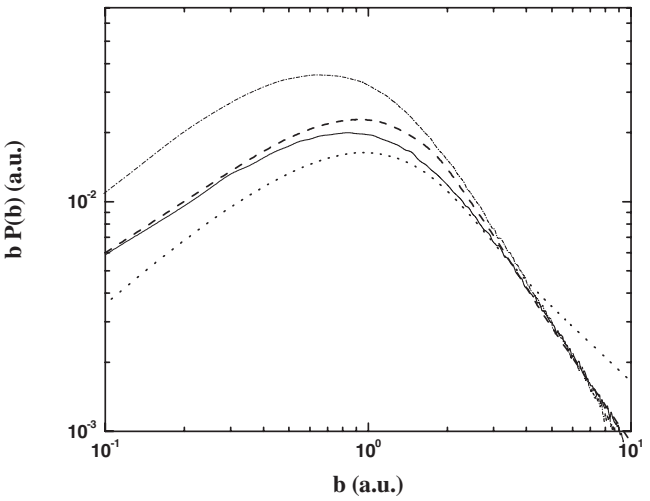

FIG. 1. Single ionization cross sections differential in impact parameter $d\sigma/db = bP(b)$ for 100 MeV/amu C^{6+}+He collisions. Solid curve, simulation using Eqs. (3) and (4) for $a = 0.5$; dash-dotted curve, same as solid curve, but $a = 1.0$; dotted curve, CDW-EIS; dashed curve; TDCC.

the simulation for $a = 0.5$ falls between the two theoretical curves and at large impact parameters it essentially follows the TDCC results.

The impact parameter determines the magnitude, but not the direction of $\mathbf{q}_{es}$. Therefore a third random number, uniformly distributed between 0 and 2π, is generated and associated with the azimuthal angle φ_p of the incoming projectile. The direction of $\mathbf{q}_{es}$ is then antiparallel to the projection of the projectile's position vector onto the azimuthal plane relative to the target nucleus. The procedure to convolute the FBA with elastic scattering can now be summarized by the following steps, which are repeatedly executed for each recorded ionization event: (1) three random numbers, each uniformly distributed, are generated. (2) From two of these random numbers the impact parameter is calculated using Eqs. (4a)–(4c) from which, in turn, the momentum transferred in the elastic scattering q_{es} is calculated with equation (1). (3) From the third random number, associated with the azimuthal projectile angle φ_p, the x and y components of q_{es} are calculated (the z component is essentially zero for elastic scattering) by

$$q_{esx} = -q_{es}\cos\varphi_p \quad \text{and} \quad q_{esy} = -q_{es}\sin\varphi_p. \tag{6}$$

(4) The q_{esx} and q_{esy} obtained from Eq. (6) are added to the corresponding components of the projectile momentum transfer and of the recoil-ion momentum obtained from the unconvoluted FBA. (5) The Cartesian momentum components are converted to spherical coordinates and the events are sorted into the fully differential angular electron spectra by setting appropriate kinematic conditions. Although the electron momentum in the original frame of reference (before the convolution) is not affected by the elastic scattering, the reference frame itself can change because it is partly defined by the scattering plane. The scattering plane, in turn,

will generally be rotated about the projectile beam axis due to the elastic scattering.

The classical treatment of elastic scattering in our convolution leads to two approximations which particularly should be kept in mind when comparing the results to the experimental data. First, in a consistent quantum-mechanical treatment the first-order amplitude (from the original FBA) should be added coherently to the second-order amplitude containing elastic scattering. However, for the very small perturbation considered here the inaccuracies introduced by the incoherent treatment in our model are not expected to be severe. Second, the impact parameter formulation of Eq. (3) is ill defined since in quantum mechanics the impact parameter is not an observable quantity. Equation (3) represents an approximation which is not expected to be valid if the momentum transfer is very small or very large [20]. On the other hand, such a formulation has been routinely and successfully used in the past (e.g., Refs. [21,22]) including for kinematic conditions comparable to those considered here [23].

IV. RESULTS AND DISCUSSION

In the following discussion the experimental data and all theoretical curves are relatively normalized to each other using the same total cross section [24]. In Fig. 2 singly differential data as a function of q_x (top) and q_y (bottom) are shown. The unconvoluted FBA (dotted curves) yields spectra which are clearly too narrow compared to the experimental data. After convoluting the FBA with elastic scattering (dashed curves) these discrepancies are significantly reduced. They remain most pronounced for $|q_x|$ and $|q_y|<0.2$ a.u. In this region the discrepancies are largely removed if the FBA is additionally convoluted with the experimental resolution (solid curves, for the remainder of the paper we refer to the simulation convoluted with both elastic scattering and the resolution as the "fully convoluted" FBA). At larger momentum transfers the effect of the resolution is much smaller and it is practically absent for $|q_x|$ and $|q_y|>0.3$ a.u. Overall, small discrepancies remain making the theoretical spectra slightly too narrow even after convoluting with both elastic scattering and the experimental resolution.

In Fig. 3 we present normalized doubly differential cross sections (DDCS) for fixed ejected electron energies of 10 eV (closed symbols) and 50 eV (open symbols) as a function of the transverse momentum transfer component. Such a presentation has recently been reported by Moshammer *et al.* [25] and revealed discrepancies, and in the case of large perturbations severe discrepancies, to existing theories. The simulations are labeled the same way as in Fig. 2. Again, the unconvoluted FBA is in poor agreement with the data for both energies. More specifically, the maximum in the DDCS is shifted to much smaller q compared to experiment. For 10 eV the convolution with elastic scattering leads to strongly improved agreement and the fully convoluted FBA is very close to the experimental data. Like in the case of the singly differential cross sections the influence of the resolution seems to have a rather small effect for $q>0.3$ a.u. For 50 eV the fully convoluted FBA also results in a considerably improved agreement between experiment and theory. However, although the agreement is respectable, it is not nearly as good as for 10 eV. More specifically, the maximum is shifted compared to the data from about 0.5 to 0.3 a.u. and in the region of the experimental maximum the simulation underestimates the data by about a factor of 2.

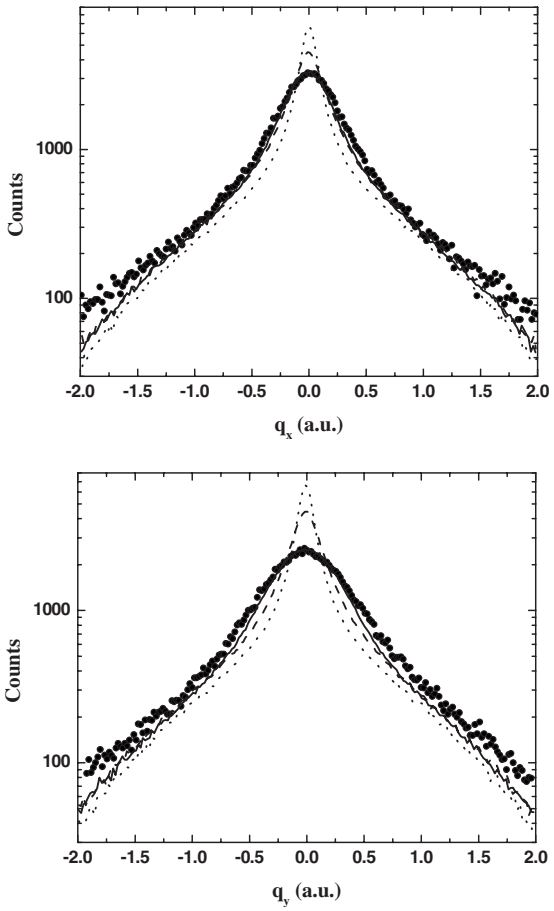

FIG. 2. Singly differential spectra as a function of the x (top) and y components (bottom) of the momentum transfer. Closed symbols, experimental data; dotted curve, unconvoluted FBA; dashed curve, FBA convoluted only with elastic scattering ($a=0.5$, see text); solid curve, FBA convoluted with both elastic scattering and experimental resolution.

Fully differential spectra are shown in Fig. 4 for electrons ejected into the scattering plane (top) and into the perpendicular plane (bottom). The ejected electron energy is fixed at $E_e=6.5\pm3.5$ eV and the momentum transfer at $q=0.75\pm0.25$ a.u. The unconvoluted FBA (dotted curves) describes the binary peak near 90° in the scattering plane very well, but the recoil peak near 270° is significantly underestimated. More seriously, as mentioned above, the FBA yields an almost isotropic angular dependence in the perpendicular plane (as expected for a first-order treatment) and does not reproduce the peak structure even qualitatively. Convoluting with elastic scattering (dashed curves) has no effect on the binary peak, but it considerably enhances the recoil peak. The peak in the perpendicular plane is now qualitatively reproduced, but is still too small compared to the data. The discrepancies between theory and experiment are further re-

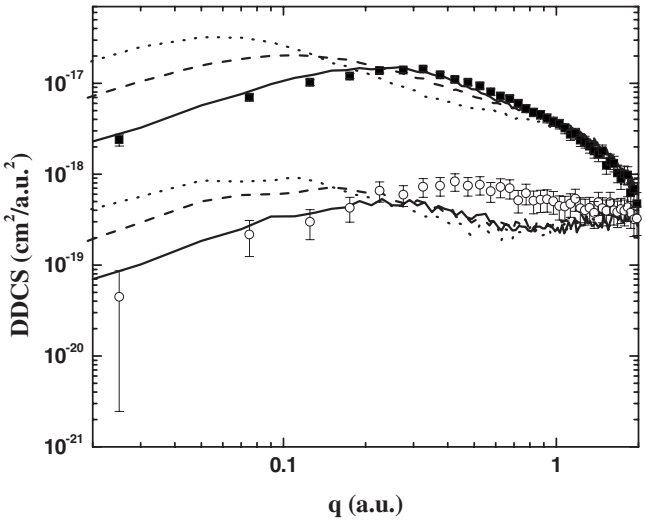

FIG. 3. Doubly differential spectra as function of the transverse momentum transfer component for electron energies of 10 eV (closed symbols) and 50 eV (open symbols). Theoretical curves as in Fig. 2.

duced by also convoluting with the resolution (solid curves). Now the agreement is good, but not perfect as both the recoil peak and the peak in the perpendicular plane are still somewhat underestimated. The FDCS are more sensitive to the resolution than the DDCS and the momentum transfer spectra, and here noticeable effects of the resolution are observed up to about $q=0.75$ a.u.

The above analysis demonstrates that indeed elastic scattering is important and can qualitatively explain the out-of-plane peak structures even at such a small perturbation as was studied here. We also note that it offers a plausible explanation for deviations between experiment and theory in the recoil peak, frequently observed for electron impact (e.g., Refs. [26,27]) as well. Nevertheless, it is, of course, desirable to understand the remaining discrepancies between the fully convoluted FBA and the present data. One possibility is that the resolution or the effects of elastic scattering are underestimated.

In our model the effect due to elastic scattering is primarily determined by the shape of $bP(b)$ and by the charge of the target core. As mentioned above, the effective b-dependent target Z of Eq. (2) represents an excellent fit to a Hartree-Fock potential and therefore its description cannot be significantly improved. The position of the maximum in $bP(b)$ can be adjusted by the parameter a in Eqs. (4a)–(4c) without changing the shape at large impact parameters. In the following we study the effect of a on the FDCS by analyzing the data for $E_e=3-50$ eV and $q=1.0-2.0$ a.u. for the perpendicular plane. As we discussed earlier [16] for large q the measured FDCS are essentially unaffected by the resolution. Therefore, for this kinematic setting we can systematically study how the effect of elastic scattering is altered by a without the analysis being obstructed by the resolution.

The FDCS for ejection into the perpendicular plane for $E_e=3-50$ eV and $q=1.0-2.0$ a.u. are shown in Fig. 5. The dashed curve is the fully convoluted FBA using $a=0.5$, i.e.,

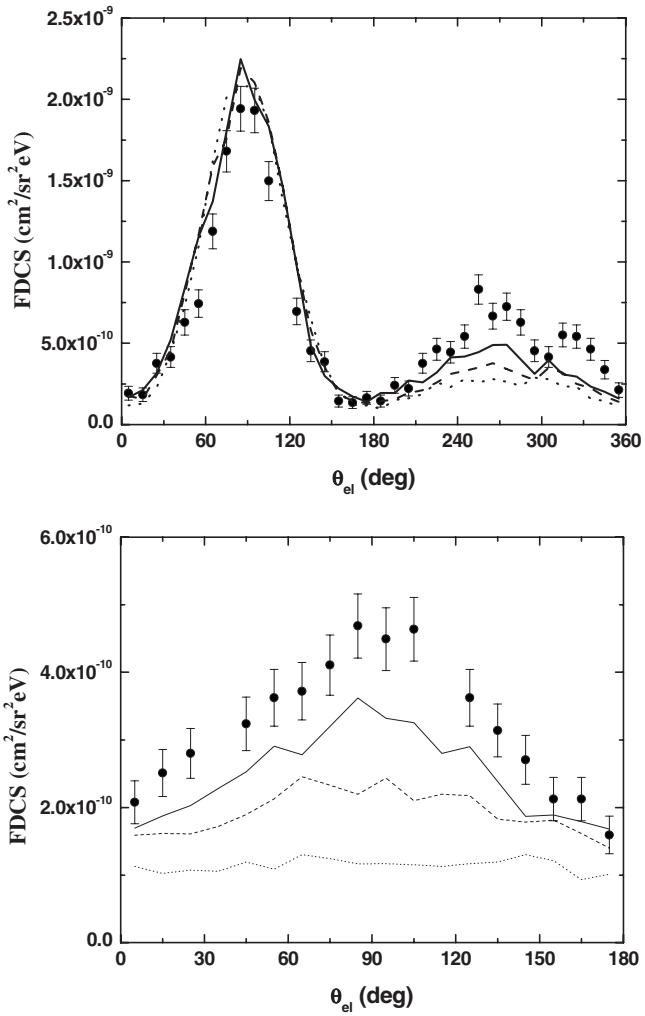

FIG. 4. Fully differential spectra for electron ejection into the scattering plane (top) and perpendicular plane (bottom). The electron energy is $E_e=6.5\pm3.5$ eV and the momentum transfer $q=0.75\pm0.25$ a.u. Theoretical curves as in Fig. 2.

the same impact parameter dependence as for the simulated FDCS of Fig. 4. For this particular value of a elastic scattering appears to be significantly underestimated. While a pronounced peak structure is observed in the experimental data, such a structure is barely discernable in the simulation. With increasing a the maximum becomes increasingly stronger. For $a=1.0$, corresponding to a maximum in $bP(b)$ at 0.7 a.u. (see Fig. 1), the experimental peak height can be well reproduced (solid curve). However, perfect agreement with the data cannot be achieved with any value of a. The width of the peak is overestimated and if a is further increased the peak height becomes too large. The solid curve in Fig. 5 ($a=1.0$) represents a best fit of the peak height to the data.

The lack of peak structure in the perpendicular plane for $E_e=3-50$ eV and $q=1.0-2.0$ for $a=0.5$ could be due to the limitations of our simulation. However, given the improved agreement with the data for $a=1.0$ and the observation that the $bP(b)$'s of different theoretical models are not identical it is also conceivable that the theoretical $bP(b)$'s indeed maximize at too large impact parameters leading to an underesti-

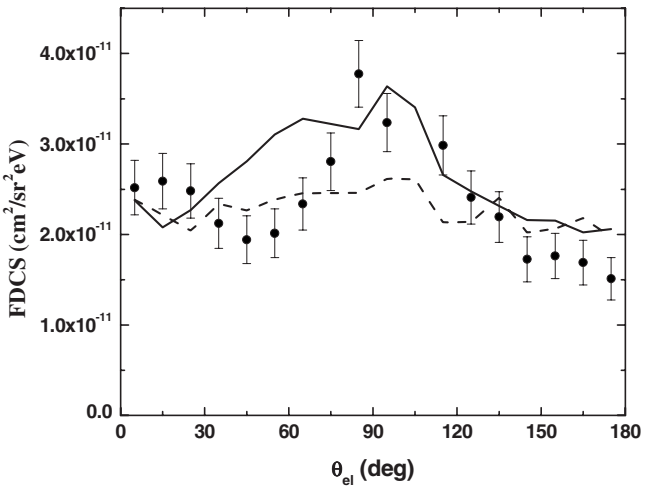

FIG. 5. Fully differential spectra for electron ejection into the perpendicular plane. The electron energy is $E_e=3-50$ eV and the momentum transfer $q=1.0-2.0$ a.u. Dashed curve, fully convoluted FBA with $a=0.5$ (see text); solid curve, fully convoluted FBA with $a=1.0$.

mation of elastic scattering. If that is the case then using $a=1.0$ should lead to an improved agreement in the FDCS for $E_e=3-10$ eV and $q=0.5-1.0$ and in the singly and doubly differential cross sections as well. In Fig. 6 the experimental data for $d\sigma/dq_x$ and $d\sigma/dq_y$ are compared to the fully convoluted FBA using $a=1.0$. Indeed, up to about ±1.5 a.u. the data are very well reproduced by the simulation. In the DDCS for $E_e=10$ eV very good agreement was readily found for $a=0.5$ (see Fig. 3). For $a=1.0$ the remaining discrepancies are further reduced; however, the change is barely noticeable on the scale of Fig. 3 (covering five decades on the ordinate). Likewise, the change in the DDCS for $E_e=50$ eV is almost not visible and the discrepancies between 0.3 and 1.0 a.u. remain. Finally, the fully convoluted FBA using $a=1.0$ reproduces the measured FDCS for $E_e=3-10$ eV and $q=0.5-1.0$ a.u. nearly perfectly, both in the scattering plane and in the perpendicular plane as can be seen in Fig. 7. Only in the recoil peak and in the angular range between 90° and 150° in the perpendicular plane the cross sections are still slightly underestimated.

Generally, surprisingly good agreement is achieved using $a=1.0$ in singly, doubly, and fully differential cross sections whenever the electron energy is less than approximately 20 eV and increasing discrepancies are found with increasing energy beyond 20 eV. These problems at larger ejected electron energies (similar observations were made for electron impact [28]) may be due to shortcomings in our model (i.e., the classical treatment of the elastic scattering). However, we note that we also find small, but nevertheless systematic, discrepancies in the singly differential cross sections as a function of electron energy above about 20 eV, for which we do not expect a strong influence of elastic scattering. It is therefore possible that the problems at large electron energies are not directly related to elastic scattering.

V. CONCLUSIONS

We have analyzed single ionization cross sections for 100 MeV/amu C^{6+}+He collisions by convoluting the first Born approximation with classical elastic scattering between the projectile and the target core using a Monte Carlo event generator technique. Peak structures in the measured fully differential cross sections for electron ejection into the perpendicular plane, which previously could not consistently be described by any theoretical model, are qualitatively reproduced.

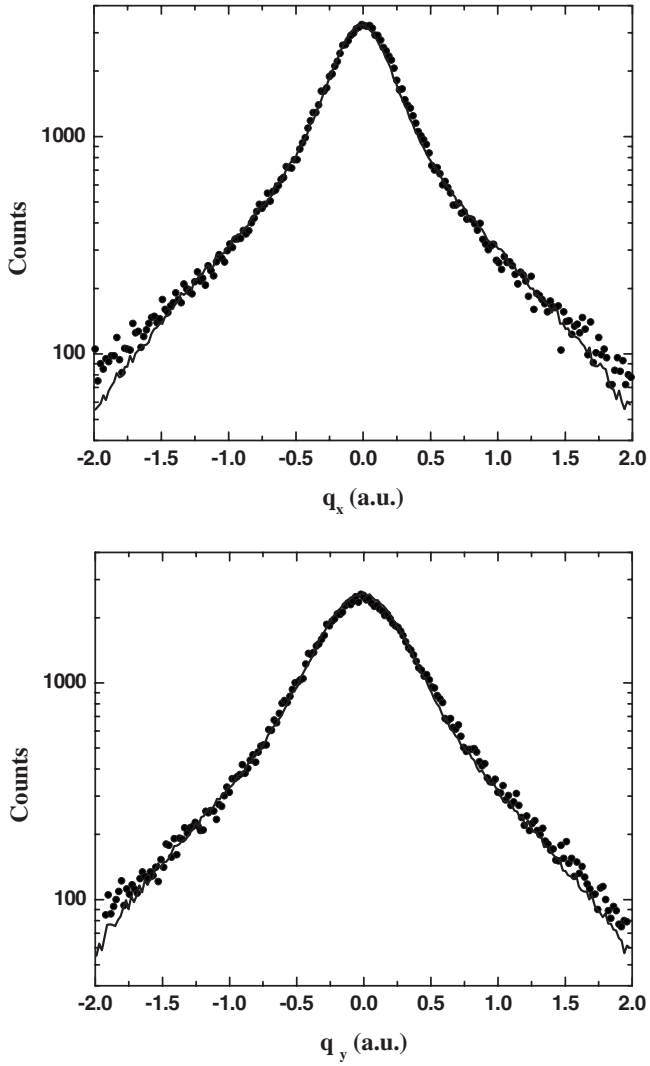

FIG. 6. Same as Fig. 2, but fully convoluted FBA is shown for $a=1.0$.

Quantitatively, the cross sections are somewhat sensitive to the shape of the $bP(b)$ used in the convolution. If an impact parameter dependence with a theoretically predicted maximum at $b=0.9$ a.u. is used, the data are underestimated by about 30% by the fully convoluted FBA. However, surprisingly good agreement is achieved if the maximum is shifted to 0.7 a.u. Singly and doubly differential cross sections are then in very good agreement as well for electron energies below about 20 eV and in reasonable agreement for larger energies. The analysis presented here therefore suggests that the peak structures in the perpendicular plane are indeed due to a higher-order process involving the projectile-target core interaction. The recoil peak appears to be significantly affected by that interaction as well.

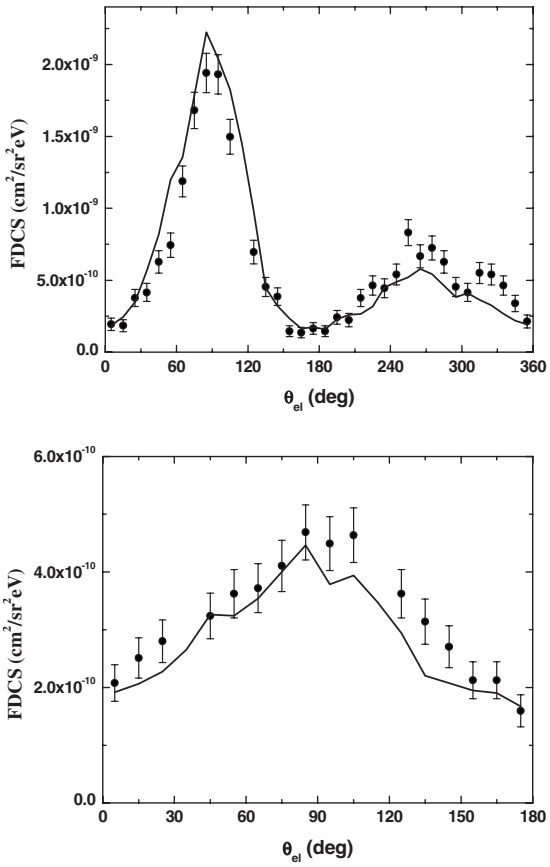

FIG. 7. Same as Fig. 4, but fully convoluted FBA is shown for $a=1.0$.

One question which needs to be answered is why more sophisticated calculations, such as, e.g., the 3DW model, are not capable of reproducing the out-of-plane structures even qualitatively. One problem with this approach has been identified already: for heavy-ion impact it is currently not feasible to describe the projectile-target core interaction in terms of a distorted wave and a Coulomb wave is used instead corresponding to a constant charge of 1 for the target core [12]. In our model, in contrast, we use an impact parameter-dependent effective charge. Further problems may result from the $bP(b)$'s in the 3DW model, which does not directly appear in the calculation, but in principle can be deduced from a Fourier transform of the q-dependent transition amplitude. Various theoretical models predict different values and our simulation demonstrates that quantitatively the FDCS are somewhat sensitive to the shape of the $bP(b)$'s. Other problems may exist and to identify them should be a subject of detailed investigations.

Perhaps the most significant prospect resulting from this work is the tremendous extension of possibilities for theoretical studies offered by the event generator technique. Often, cross sections which can be extracted from kinematically complete experiments cannot be easily calculated using conventional methods because the conversion of the transition amplitudes to the measured cross section is not always straightforward. For example, lack of symmetry may require intensive numeric integration which can make the computation unfeasible. On the other hand, with the event generator technique any differential data that can be extracted from experiment may be simulated from the theory because the theoretical event file has exactly the same structure as the experimental event file. To generate the event file can be very time consuming; however, once it has been generated any cross section can be extracted within approximately one minute on a laptop. Another big advantage is that the experimental resolution and instrumental acceptances can be incorporated so that a direct comparison with experiment becomes possible. We are currently applying this technique to calculations of "unconventional" double ionization spectra which so far were impossible to calculate.

ACKNOWLEDGMENTS

We would like to thank Dr. T. Kirchner, Dr. L. Gulyas, and Dr. M. Foster for providing us with their theoretical $bP(b)$ and Dr. A. Voitkiv for assistance in generating the event file. This work was supported by the Deutsche Forschungsgemeinschaft and the National Science Foundation under Grant no. PHY-0353532.

[1] H. Ehrhardt, K. Jung, G. Knoth, and P. Schlemmer, Z. Phys. D: At., Mol. Clusters **1**, 3 (1986), and references therein.
[2] M. Schulz and D. H. Madison, Int. J. Mod. Phys. A **21**, 3649 (2006), and references therein.
[3] H. Ehrhardt, M. Schulz, T. Tekaat, and K. Willmann, Phys. Rev. Lett. **22**, 89 (1969).
[4] G. Stefani, L. Avaldi, and R. Camilloni, J. Phys. B **23**, L227 (1990).
[5] J. Röder, H. Ehrhardt, I. Bray, D. V. Fursa, and I. E. McCarthy, J. Phys. B **29**, 2103 (1996).
[6] M. Schulz, R. Moshammer, D. Fischer, H. Kollmus, D. H. Madison, S. Jones, and J. Ullrich, Nature (London) **422**, 48 (2003).
[7] M. Schulz, R. Moshammer, A. N. Perumal, and J. Ullrich, J. Phys. B **35**, L161 (2002).
[8] N. V. Maydanyuk, A. Hasan, M. Foster, B. Tooke, E. Nanni, D. H. Madison, and M. Schulz, Phys. Rev. Lett. **94**, 243201 (2005).
[9] M. Dürr, C. Dimopoulou, B. Najjari, A. Dorn, and J. Ullrich, Phys. Rev. Lett. **96**, 243202 (2006).
[10] E. Y. Kamber, C. L. Cocke, S. Cheng, and S. L. Varghese, Phys. Rev. Lett. **60**, 2026 (1988).
[11] D. H. Madison, D. Fischer, M. Foster, M. Schulz, R. Moshammer, S. Jones, and J. Ullrich, Phys. Rev. Lett. **91**, 253201 (2003).
[12] M. Foster, J. L. Peacher, M. Schulz, D. H. Madison, Zhangjin Chen, and H. R. J. Walters, Phys. Rev. Lett. **97**, 093202 (2006).

[13] A. B. Voitkiv, B. Najjari, and J. Ullrich, J. Phys. B **36**, 2591 (2003).
[14] J. Fiol and R. E. Olson, J. Phys. B **37**, 3947 (2004).
[15] J. Fiol, S. Otranto, and R. E. Olson, J. Phys. B **39**, L285 (2006).
[16] M. Dürr, B. Najjari, M. Schulz, A. Dorn, R. Moshammer, A. B. Voitkiv, and J. Ullrich, Phys. Rev. A **75**, 062708 (2007).
[17] F. Martin and A. Salin, Phys. Rev. A **55**, 2004 (1997).
[18] P. D. Fainstein and L. Gulyas, Nucl. Instrum. Methods Phys. Res. B **235**, 306 (2005).
[19] M. S. Pindzola, T. G. Lee, T. Minami, and D. R. Schultz, Phys. Rev. A **72**, 062703 (2005).
[20] P. T. Greenland, J. Phys. B **14**, 3707 (1981).
[21] L. Kocbach, J. M. Hansteen, and R. Gundersen, Nucl. Instrum. Methods **169**, 281 (1980).
[22] T. Kirchner, M. Horbatsch, and H. J. Lüdde, J. Phys. B **37**, 2379 (2004).
[23] M. Horbatsch, J. Phys. B **22**, L639 (1989).
[24] D. H. Madison, M. Schulz, S. Jones, M. Foster, R. Moshammer, and J. Ullrich, J. Phys. B **35**, 3297 (2002).
[25] R. Moshammer, A. N. Perumal, M. Schulz, V. D. Rodriguez, H. Kollmus, R. Mann, S. Hagmann, and J. Ullrich, Phys. Rev. Lett. **87**, 223201 (2001).
[26] P. Marchalant, C. T. Whelan, and H. R. J. Walters, J. Phys. B **31**, 1141 (1998).
[27] S. Jones and D. H. Madison, Phys. Rev. Lett. **81**, 2886 (1998).
[28] F. Catoire, E. M. Staicu-Casagrande, M. Nekkab, C. Dal Cappello, K. Bartschat, and A. Lahmam-Bennani, J. Phys. B **39**, 2827 (2006).